This document is the Accepted Manuscript version of N. Otegi, J. -M. Collantes, I. Lizarraga, J. M. Gonzalez "Characterization Technique to Reveal Critical Resonances in Nonlinear RF Circuits," in *IEEE Transactions on Instrumentation and Measurement*, vol. 71, pp. 1-11, 2022, Art no. 8003211, doi: 10.1109/TIM.2022.3170883.

The Final Published version is available online via https://ieeexplore.ieee.org/document/9764705.

Characterization Technique to Reveal Critical Resonances in Non-linear RF Circuits

Nerea Otegi, Juan-Mari Collantes, Ibone Lizarraga, Jose Manuel Gonzalez

***Abstract*— The presence of critical resonances can significantly impact the stable and robust operation of microwave amplifiers, leading to spurious oscillations in the worst case. In this work, a technique based on noise measurements performed with a spectrum analyzer is presented to experimentally characterize these resonances. Broadband white noise is injected to the input of the circuit so the critical resonances are clearly revealed above the noise floor of the measuring instrument, without the need of exigent settings and far from the bifurcation point. In addition to detecting potentially risky resonances, the actual position of the critical poles on the pole-zero map can be estimated from these noise measurements applying pole-zero identification techniques. The noise injection technique has been tested in two non-linear prototypes in microstrip technology: an analog frequency divider and an L-band amplifier.**

***Index Terms*— Circuit stability, resonances, noisy precursor, poles and zeros, stability margin.**

I. Introduction

Non-linear RF and microwave circuits are prone to exhibit unstable behavior that can be revealed as autonomous oscillations [1]-[4] that are function of the input power. This is the case of power amplifiers, which typically operate at substantial compression levels to reach acceptable efficiency values, or analog frequency dividers that need a large-signal input drive to generate a parametric oscillation. In some cases, input power may lead the non-linear system to a bifurcation point, following which a qualitative change in its behavior is observed. Indeed, the presence of critical resonances that shift with input power is one of the main risks for the stable and robust operation of microwave power amplifiers. These resonances, although stable, are characterized by the presence of complex conjugate poles with very low damping (small real part) and they affect circuit performances [5], [6]. Small stability margins make power amplifiers very sensitive against changes (bias, temperature, load impedance, aging, etc.). Consequently, a power amplifier can easily end up showing a spurious oscillation if its operating conditions are modified [7]. In addition, poles with low damping factors can generate other problems in power amplifiers. When these resonances occur at low frequencies, they are responsible for the appearance of transient responses in pulses, affecting the pulse profile in radar applications [8]. These low-frequency resonances have also a direct impact on the amplifiers' video bandwidth, limiting the effectiveness of digital pre-distortion systems [9], [10].

Identification of the system poles is a useful tool to understand the circuit dynamics. Their knowledge is important at the time of redesigning and fixing the circuit to avoid low stability margins. The experimental identification of the poles can either corroborate simulation results and confirm the reliability of the electrical models, or reveal critical dynamics that were not correctly modeled in the electrical description of the circuit. In this second case, results can be used to improve device models through a back simulation process in order to enhance their prediction capabilities.

Therefore, it is essential to detect the critical dynamics at early stages of the prototype development in order to correct it efficiently, improving the robustness and reliability of the final circuit. Several techniques are proposed in the literature to characterize different aspects of the non-linear dynamics in microwave active circuits. Experimental techniques are a good complement to electrical circuit simulations, particularly when non-linear active models are not fully reliable or when parts of the system are not perfectly modeled (thermal effects, bias circuitry, etc.). In [11], the auxiliary generator technique is adapted to the experimental measure of the bifurcation curves of several non-linear circuits. An active bias network is presented in [12] to characterize the low-frequency dispersion in the output impedance of high-power microwave transistors. A characterization of the non-linear impedance functions at the supply terminals of envelope tracking amplifiers through multitone signals is presented in [13]. In [14], the frequency response of the output power and gain of an RF power amplifier are monitored by thermal imaging. A multiport system for the measurement of complex distortion in non-linear microwave circuits is presented in [15]. Multisine excitations are applied in [16], [17] to quantify the level of the distortion in low-frequency weakly non-linear time-varying systems.

Experimental characterization techniques to detect critical resonances that can lead the power amplifier to oscillate are presented in [7]. Critical poles were obtained from reflective

Manuscript submitted October 15, 2021

This work was supported by the Spanish Administration under Project PID2019-104820RB-I00.

Nerea Otegi, Juan-Mari Collantes and Ibone Lizarraga are with Departamento de Electricidad y Electrónica, Universidad del País Vasco / Euskal Herriko Unibertsitatea, UPV/EHU, Bilbao, 48080, Spain (e-mail: nerea.otegi@ehu.eus; juanmari.collantes@ehu.eus; ibone.lizarraga@ehu.eus)

Jose Manuel Gonzalez is with the Departamento de Tecnología Electrónica, Universidad del País Vasco / Euskal Herriko Unibertsitatea, UPV/EHU, 01006, Vitoria-Gasteiz, Spain (e-mail: jmgonzalezp@ehu.eus)

measurements using a vector network analyzer. However, poles outside the amplifier's bandwidth are difficult to extract due to a lack of sensitivity. To solve this drawback, extra RF ports were inserted in the bias lines of the amplifier to detect low-frequency critical resonances in [18]. The problem with this approach is that the insertion of the extra ports needs to be foreseen at the moment of designing the layout of the circuit. Besides, adding extra ports can be cumbersome for multistage power amplifiers. To avoid the presence of these extra-ports, the technique is adapted in [19] to obtain the critical poles at internal nodes of the circuit using high-impedance probes. Results are satisfactory for low-frequency resonances. However, due to the perturbing effect of the probes it is hardly extendable to high frequencies. For the same reason, when the power amplifier is working in large-signal operation, it can only be implemented at those nodes that are decoupled from the RF signal. This limits the applicability of the high impedance probing technique considerably.

An innovative approach that makes use of electro-optic probes to detect internal oscillations in high power amplifiers is presented in [20], [21]. The advantage of using electro-optic probes is the possibility to ensure that the circuit is not being perturbed during the characterization. However, this approach can only be applied once the oscillation has taken place. It is useful to reveal the presence and understand the nature of oscillations in parallel power structures but it cannot provide a measure of the stability margins before the bifurcation happens.

In this work a different solution is implemented to estimate experimentally the stability margins of critical resonances with the circuit operating in large signal. The idea is to use the measured output noise spectrum of the system to characterize critical resonances.

Low-damping complex-conjugate poles are responsible for the presence of noise bumps in the output spectrum of active circuits [3], [22], [23]. The steady-state solution of the system is continuously perturbed by the noise sources, generating transients at the frequency of the dominant low-damping poles. This effect can be observed in the spectrum as an increase of the noise around the frequency of the critical poles. This noise bump can turn into a discrete spectral line if the poles cross to the Right Half Plane (RHP) when a circuit parameter is varied. This kind of noise raise that precedes the oscillation as a circuit parameter varies is often called noisy precursor [3].

In theory, searching for noisy precursors in the spectrum could be an indirect sensing method to detect low-damping critical poles and thus, low stability margins in a circuit. However, noisy precursors are not always easily observable. If the gain from the noise sources to the output of the circuit is low, the noisy precursor will be masked under the noise floor of the measurement test bench [3].

The approach presented here is based on injecting broadband white noise at the input of the circuit so that the effect of the low-damping poles on the output noise spectrum can be observed without requiring measurement setups with stringent noise floor performances. From simple noise power measurements at the spectrum analyzer we will be able to characterize the critical dynamics of the circuit. A specific method is developed to extract the position of the critical poles on the complex plane from the scalar measurements without the need of using vector measurements obtained at extra RF ports or from high impedance probes as in [18], [19].

The paper is organized as follows. In section II the fundamental theory describing the origin of noisy precursors is explained, together with a method to obtain the critical poles from scalar measurements. The measurement setup is detailed in section III. In section IV two different application examples are presented to demonstrate the technique. A discussion with the main advantages and limitations of the technique is included in section V.

II. THEORY

A. Noisy precursors

A nonlinear system can be described by a state-space equation of the form:

$$\dot{\bar{x}} = f_{nl}(\bar{x}) \tag{1}$$

where $\bar{x}$ is the state vector and f_{nl} is a nonlinear function. If $\bar{x}_0(t)$ is a periodic steady-state solution of (1) with period $T = 1/f_0$, the dynamics of a small-signal perturbation $\bar{\xi}(t)$ applied around the periodic solution $\bar{x}_0(t)$ is described by the linearized system around $\bar{x}_0(t)$:

$$\dot{\bar{\xi}}(t) = Jf\big(\bar{x}_0(t)\big)\bar{\xi}(t) \tag{2}$$

with $Jf\big(\bar{x}_0(t)\big)$ being a periodic jacobian matrix. Equation (2) represents a Periodic Linear Time Variant (PLTV) system and its solution has the form:

$$\bar{\xi}(t) = c_1 e^{\lambda_1 t}\bar{v}_1(t) + c_2 e^{\lambda_2 t}\bar{v}_2(t) + \cdots + c_n e^{\lambda_n t}\bar{v}_n(t) \tag{3}$$

where n is the order of the system, $c_1, \cdots, c_n$ are constants that depend on the initial conditions, $\bar{v}_1(t), \cdots, \bar{v}_n(t)$ are periodic vectors and $\lambda_1, \cdots, \lambda_n$ are the real or complex conjugate Floquet exponents that define the asymptotic behavior of the solution. The imaginary part of each Floquet exponent is repeated periodically with ω_0: $\lambda_i \pm jk\omega_0$, where k is a positive integer. If an input/output Laplace representation of the system in (2) is considered, Floquet exponents agree with the poles of the resulting harmonic transfer function [24], [25]. Since the noise can be considered as a perturbation of the system around the periodic steady state, the Floquet exponents (or the system poles) have a direct influence on the noise amplitude spectrum. Let us consider a pair of low-damping dominant complex-conjugate poles of the system, $\sigma_d \pm j\omega_d$. Due to the periodicity of the system, these poles are repeated with ω_0 like the Floquet exponents: $\sigma_d \pm j\omega_d \pm jk\omega_0$. As explained in [3], [26], the noise spectrum near ω_d and sideband frequencies $k\omega_0 \pm \omega_d$, can be approximated to:

$$\begin{aligned} S(\omega)|_{around\ \omega_d} &= \frac{C_0(\omega)}{\sigma_d^2 + (\omega - \omega_d)^2} \\ S(\omega)|_{around\ k\omega_0+\omega_d} &= \frac{C_{k+}(\omega)}{\sigma_d^2 + (\omega - k\omega_0 - \omega_d)^2} \\ S(\omega)|_{around\ k\omega_0-\omega_d} &= \frac{C_{k-}(\omega)}{\sigma_d^2 + (\omega - k\omega_0 + \omega_d)^2} \end{aligned} \tag{4}$$

The terms in the numerators of expressions (4) $C_k(\omega)$ are related to the amplitude of the noise sources and their conversion gains to the output port at which the noise is calculated or measured. Note that expressions (4) are only valid if there are no other low-damping poles at frequencies nearby. If that were the case, a joint contribution should be considered. Assuming white noise inputs, expressions (4) predict a set of Lorentzian lines centered at $\omega_d, \omega_0 \pm \omega_d, 2\omega_0 \pm \omega_d$, and so on. The smaller the absolute value of the negative real part of the poles $|\sigma_d|$, the larger the amplitude of the resonant peaks. This is observed in the noise spectrum as noise bumps centered at those frequencies. As an example, Fig. 1a shows a noise bump that is observed in an analog frequency divider just before the bifurcation takes place. If when varying a circuit parameter the real part of the poles shifts rightwards on the complex plane and eventually happens to cross to the right half plane, the bifurcation takes place and the bump turns into a distinct spectral line. This is shown in Fig. 1b. Since the noise bump precedes the oscillation, it is generally called noisy precursor. In practice, however, the noisy precursors are not always observable in the measured output spectrum of the circuit. Depending on the conversion gain characteristics from the noise sources to the output port, the noise bumps may remain hidden under the noise floor of the measurement system. In most practical cases, only when the absolute value of the negative real part $|\sigma_d|$ is extremely small (very low-damping poles, the system is very close to the bifurcation point) we will be able to observe noise bumps in the output spectrum, although not necessarily at all the frequencies $\omega_d, k\omega_0 \pm \omega_d$.

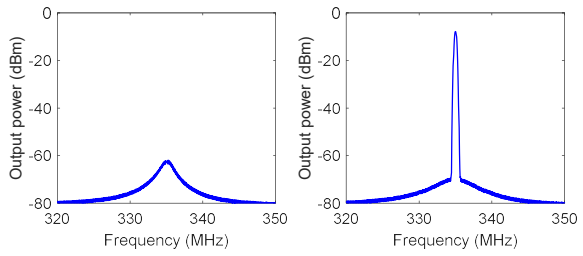

Fig. 1. Measured output spectrum of a frequency divider around the divided frequency $f_0/2$: a) noise bump measured just before bifurcation; b) spectral line at divided frequency after bifurcation.

In this work, we propose an experimental technique to increase the level of the noise bumps by injecting broadband noise at the input of the device. The idea is to enhance the noise bumps so that at least one of terms of (4) raises above the noise floor of the measurement setup. This will allow the detection of the critical resonances even when the system is not extremely near the bifurcation point. Output results will be scalar power measurements carried out in a spectrum analyzer.

B. Identification of the system poles from scalar measurements

The system poles of a PLTV system, that are equivalent to the Floquet exponents of (3), can be obtained from a single-input single-output transfer function element of the harmonic transfer function matrix [24]. This is a process that is commonly used in power amplifier design to analyze the stability of large-signal periodic regimes obtained with harmonic balance simulators [4] and is called pole-zero identification stability analysis [27]. The method is based on analyzing a frequency response, $H(j\omega)$, of the circuit linearized around a periodic steady state forced by the large-signal input. The frequency response is computed through a large-signal/small-signal harmonic balance simulation using a conversion matrix algorithm. Next, frequency domain identification techniques for linear systems are applied to $H(j\omega)$ in order to obtain the corresponding transfer function in the Laplace domain $H(s)$. System poles are directly given by the denominator of $H(s)$. In simulation, typical frequency responses for stability analysis are impedances at internal circuit nodes or admittances at circuit branches. Other input/output representations are possible, such as transimpedances, transadmittances, or voltage and current transfers, because all the transfer functions associated to a linearized system share the same characteristic equation, i.e. the same set of poles.

When dealing with an experimental characterization of the stability margins in a power amplifier, impedances at internal circuit nodes or admittances at circuit branches cannot be practically measured. Instead, other types of frequency responses are measured. In [18], the low-frequency critical poles are identified from reflection coefficients measured at extra ports inserted in the bias lines of the amplifier. In [19], a voltage transfer function was used to identify the poles from voltages obtained at different nodes with a high impedance probe. A common feature of all these approaches, either in simulation or measurement, is that the frequency responses are complex quantities. Indeed, pole-zero identification algorithms require both magnitude and phase of $H(j\omega)$ to correctly approximate the transfer function $H(s)$.

However, in our case, scalar power measurements at the spectrum analyzer are obtained as unique outcome. No phase information is available for pole-zero identification. Therefore, a specific method is proposed in the following to estimate the actual position of the critical poles on the complex plane from the noise power measurements.

Let us consider a generic stable transfer function $H_1(s)$ with a particular pole-zero map given by the blue poles and zeros of Fig. 2.

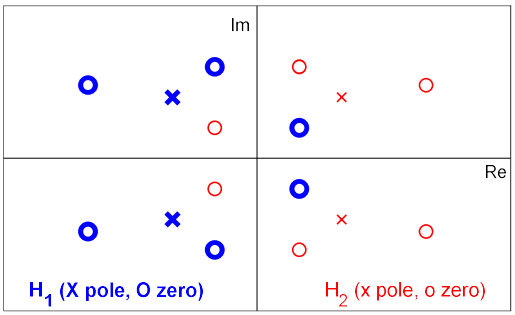

Fig. 2. Pole-zero maps of generic transfer functions H_1 (blue) and H_2 (red). Poles and zeroes of both transfer functions are symmetrically located with respect to imaginary axis.

Superimposed in red in Fig. 2 is the pole-zero map of a second transfer function $H_2(s)$, whose poles and zeros are

symmetrically located with respect to the imaginary axis. Poles and zeros of H_2(s) have the same imaginary part than those of H_1(s) but opposite real part. Their frequency responses have the same magnitude and opposite phase:

$$H_1(j\omega) = |H|e^{j\varphi} \quad (5)$$
$$H_2(j\omega) = |H|e^{-j\varphi} \quad (6)$$

The multiplication of $H_1(j\omega)$ by $H_2(j\omega)$ creates a frequency response $G(j\omega)$ with zero phase:

$$G(j\omega) = |H|^2 e^{j0} \quad (7)$$

The poles of $G(s)$ comprise the joint set of poles of $H_1(s)$ and $H_2(s)$. Note that, if $H_1(s)$ is a stable transfer function, the Left Half Plane (LHP) poles of $G(s)$ are the complete set of poles of $H_1(s)$. We will use this feature to estimate the poles of the DUT from the broadband noise power measurements.

Let us consider here a voltage transfer function like in [19]. This voltage transfer function relates the output voltage of the DUT, v_{out}, to the voltage of an external generator connected at its input, v_{gen} (Fig. 3). Considering the complex phasors of these voltages, $V_{out}(j\omega)$ and $V_{gen}(j\omega)$, the frequency response will be:

$$H(j\omega) = \frac{V_{out}(j\omega)}{V_{gen}(j\omega)} \quad (8)$$

The squared magnitude of H becomes:

$$|H(j\omega)|^2 = \frac{|V_{out}(j\omega)|^2}{|V_{gen}(j\omega)|^2} \quad (9)$$

which is proportional to the ratio of the power at the output of the DUT over the power injected from the generator. We can obtain a good approximation of $|H(j\omega)|^2$ using a broadband noise excitation. For that, we need to inject noise power practically flat along the measurement band so it can be considered constant in frequency. Assuming the internal noise added by the active DUT is negligible for the values of the injected noise, then $|H(j\omega)|^2$ is simply proportional to the noise power measured by the spectrum analyzer N_{out} along the measurement frequency band:

$$|H(j2\pi f)|^2 = K\, N_{out}(f) \quad (10)$$

where K is a constant with no influence in the position of the poles and zeros.

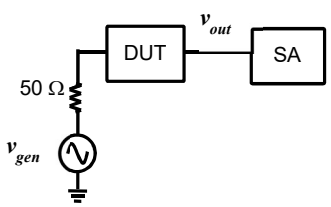

Fig. 3. Basic block-diagram for voltage transfer function obtaining.

Thus, we can use the noise power measured by the spectrum analyzer along the measurement frequency band $N_{out}(f)$ to build a zero-phase frequency response:

$$G(f) = N_{out}(f)e^{j0} \quad (11)$$

Applying pole-zero identification to $G(f)$ will provide a pole-zero map with symmetrical poles and zeros, like the one in Fig. 2. Since $H(s)$ is a stable linear transfer function (any steady state experimentally measured in the laboratory gives rise to a stable transfer function because it is physically observable [3]), the LHP poles of $G(s)$ will directly correspond to the poles of $H(s)$, as explained above.

In this way, we can use the measured noise spectrum at the output of the DUT to identify the position of the critical poles and their evolution versus critical parameters.

III. Experimental Setup

To generate the required broadband noise levels, a variable noise generator has been implemented using a Keysight 346B noise source and variable amplification (Fig. 4). Note that a 50 Ω termination could be used to generate thermal noise. However, the 346B noise source is used as it provides 15 dB of extra noise power with respect to a 50 Ω load at the reference temperature. For the variable amplification, a chain of commercial amplifiers and variable attenuators have been used. It is important that this chain behaves linearly and does not present resonances that may distort the characterization of the noisy precursors. In our setup, noise power levels can be generated from -174 dBm/Hz up to -90 dBm/Hz in steps of 1dB. Power variations versus frequency are less than 2 dBm along the 10 MHz – 1 GHz bandwidth. This flat bandwidth is good enough to characterize the resonances in the application examples that are shown in this work, but it could be easily extended if needed using amplifiers with wider bandwidths. The noise measurements have been performed with an ESA E4440A spectrum analyzer (SA).

To analyze critical resonances associated to large-signal operation, a driving signal is required at the input of the device. Thus, a power combiner is used to combine the driving signal at the input frequency with the noise generator. A basic block diagram of the measurement setup can be seen in Fig. 4. A photograph of the experimental setup can be seen in Fig. 4b.

If the driving signal is not needed, because we want to characterize resonances associated to a dc regime for instance, the noise generator would be directly connected to the input of the DUT. In the absence of large-signal drive, the setup could be comparable to the noise calibration of a linear receiver as in radiometry applications [28], [29]. Radiometers require ultra linear and temperature-stable gains that can be calibrated with broadband noise sources at known temperatures. Note that, in the proposed approach, the noise source is not used for calibration but for enhancing the noise bump above the noise floor. Consequently, the knowledge of the actual temperature of the noise source is irrelevant in this case.

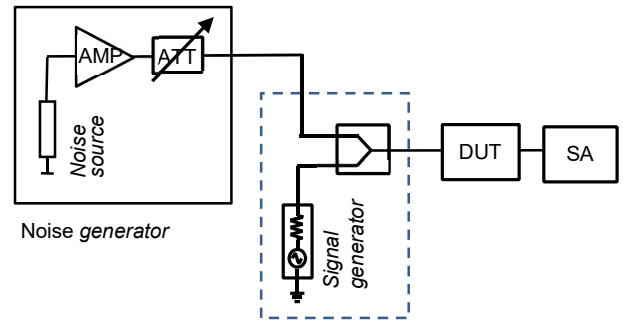

a)

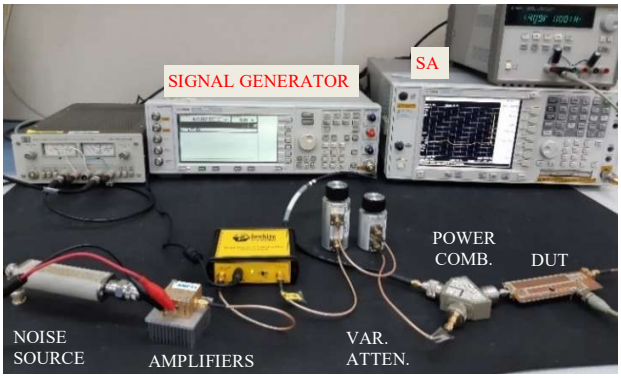

b)

Fig. 4. Implemented measurement setup: pumping signal from signal generator and broadband noise from noise generator are combined at the input of the DUT and a spectrum analyzer measures the output power: a) Basic block-diagram; b) Photograph.

IV. Application Examples

Two different circuits will be used to show the proposed methodology: a varactor-based frequency divider and an RF L-band amplifier. In both cases, characterization considers large-signal regimes with the input power drive applied to the circuit. Both circuits are built in microstrip hybrid technology with the purpose of illustrating and validating the technique.

A. Frequency Divider

The first example is a frequency divider fabricated in hybrid technology using a SMV1255 varactor. Input frequency is 670 MHz and the circuit divides the frequency by a factor of 2 for input power larger than 11 dBm, with a -1.9 V bias. This is a convenient test device because it is a simple circuit whose critical poles can be determined through an independent measurement technique [7]. In this way, we have a reference with which we can validate the results obtained from the noise characterization. Fig. 5 shows a photograph of the circuit.

To characterize its critical poles, pole-zero identification has been applied to a measured frequency response following the technique in [7]. The reflection coefficient at the output port is measured along the characterization band with a vector network analyzer while the input signal (at 670 MHz) is applied at the input port. The measured reflection coefficient is then used to compute an admittance function that represents the total admittance seen by an ideal voltage source connected in series at the output port, as we would do in a conventional stability analysis in simulation. Next, the admittance function is identified using a commercial pole-zero identification tool [30].

These measurements have been performed for different power levels below the bifurcation point (i. e. $P_{in} < 11$ dBm). The obtained critical poles with the divider biased at -1.9 V are given in Fig. 6. For clarity, only the poles with positive imaginary part are plotted in Fig. 6. Two pairs of complex conjugate dominant poles, corresponding to an input power P_{in} of 0 dBm, can be seen in Fig. 6a. The frequencies of these poles are 570 MHz and 335 MHz. The evolution of these two poles versus P_{in} is plotted in Fig. 6b. The poles at 570 MHz are not significantly affected by input power. The poles at 335 MHz move rightwards versus P_{in}, finally crossing to the RHP and leading to the autonomous spectral line at the divided frequency, as seen in Fig. 1b. These poles, obtained using [7], are used as a benchmark to assess the results of the proposed technique based on noise injection.

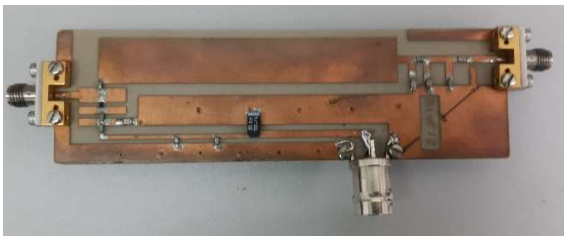

Fig. 5. Photograph of frequency divider fabricated in hybrid technology using an SMV1255 varactor.

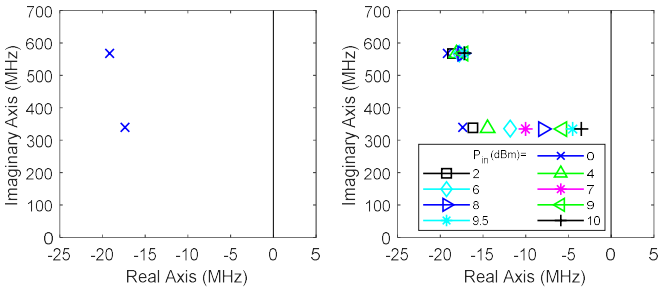

a) b)

Fig. 6. Critical poles measured using the technique proposed in [7]. a) Two pairs of complex conjugate dominant poles measured for input power of 0 dBm; b) Evolution of poles with increasing input power from 0 to 10 dBm: critical poles at divided frequency approaching to RHP while poles at 570 MHz remain almost unaffected. Only positive frequencies of the complex plane are plotted.

The proposed noise injection method has been applied to the frequency divider. An input signal of $P_{in} = 0$ dBm, $f_{in} = 670$ MHz is applied to port 1 of the combiner while the variable noise generator is connected to port 2. To begin with, a measurement of the output power spectrum is performed with the noise generator, noise source plus amplifier chain, switched off. We will call it "cold" measurement. This is equivalent to a conventional measurement with only thermal noise corresponding to a 50 Ω load at ambient temperature connected at the input of the circuit, i.e. -174 dBm/Hz noise injected. The measurement is performed with a spectrum analyzer using a resolution bandwidth of 1 MHz. The result corresponds to the

bottom trace in Fig. 7 and as it can be seen, only the spectral line at fin is visible in the spectrum.

Next, the noise generator is switched on and different noise levels are injected at port 2 of the combiner. Note that the signal generator connected at port 1 is still applying the input drive to the circuit (P_{in} = 0 dBm and f_{in} = 670 MHz). As input noise is increased, two noise bumps start emerging from the instrument noise floor. This can be observed in the middle trace of Fig. 7, which shows the measured output spectrum for an input noise level of -130 dBm/Hz. The injected noise level will always be given at the input of the power combiner. It can also be expressed as an Excess-to-Noise Ratio –ENR- with respect to the "cold" measurement (ENR of 44 dB in this case). One noise bump is revealed around the divided frequency (335 MHz) and the other one around 570 MHz. Increasing the input noise level, the noise bumps are more clearly noticeable in the spectrum, as shown by the upper trace of Fig. 7, where an input noise of -120 dBm/Hz (ENR = 54 dB) is applied. The presence of these two noise bumps perfectly correlates with the resonances associated to the measured poles depicted in Fig. 6a.

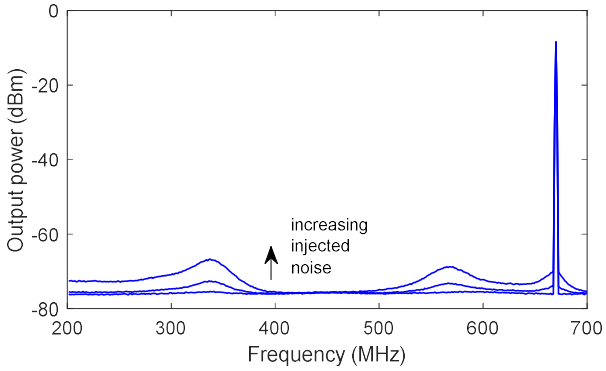

Fig. 7. Output spectrum of frequency divider with 0 dBm input signal and three different input noise levels: -174 dBm/Hz (cold measurement), -130 dBm/Hz and -120 dBm/Hz.

The evolution of these "noise resonances" while varying a circuit parameter can also be studied with this characterization setup. Let us take for instance the upper output spectrum shown in Fig. 7 and see its evolution as a function of input power. The input noise level is maintained at -120 dBm/Hz (ENR = 54 dB) and the input power P_{in} is increased from 0 dBm to 10 dBm (just below the bifurcation point). The obtained results are depicted in Fig. 8 and they reproduce the behavior expected from the measured poles of Fig. 6b. The noise bump at 570 MHz remains unchanged while the one at the divided frequency (335 MHz) grows and sharpens with increasing input power. Obviously, for P_{in} > 11 dBm the noise bump turns into a spectral line as in Fig. 1b and the circuit divides its frequency by 2.

The extra noise added by the noise generator serves to reveal the existence of critical resonances otherwise hidden by the instrument noise floor. This is clearly observed comparing the result of the cold measurement, bottom trace in Fig. 7 with the results with noise injection in Fig. 7. To detect the resonance in the output spectrum of a conventional cold measurement (thermal noise of a 50 Ω load at ambient temperature connected at the input), the circuit has to be driven much closer to the bifurcation point. See for instance Fig. 9a and Fig. 9b where cold measurements (solid lines) are compared to the results of injecting an extra noise of -120 dBm/Hz (ENR = 54 dB) with the proposed technique (dashed lines). In Fig. 9a, P_{in} is 6 dBm and the noise bumps are barely visible in the spectrum of cold measurements (solid line). We need to be much closer to the bifurcation (P_{in} = 9 dBm) to distinctly see the noisy precursor at the divided frequency (solid line Fig. 9b). However, the two resonances are easily identified far from the bifurcation point when the extra noise is injected (dashed lines).

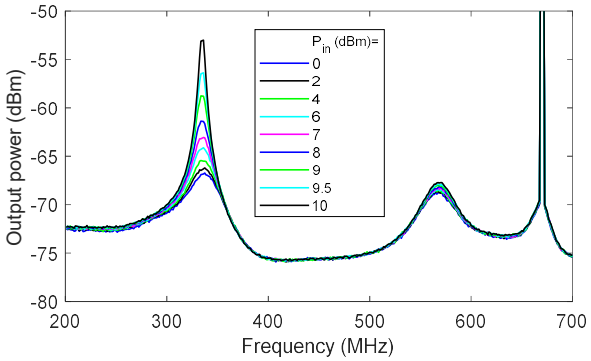

Fig. 8. Output spectrum of frequency divider with increasing input power from 0 to 10 dBm while constant broadband noise of -120 dBm/Hz is injected: growing and sharpening resonance at divided frequency and resonance unaffected by input signal at 570 MHz.

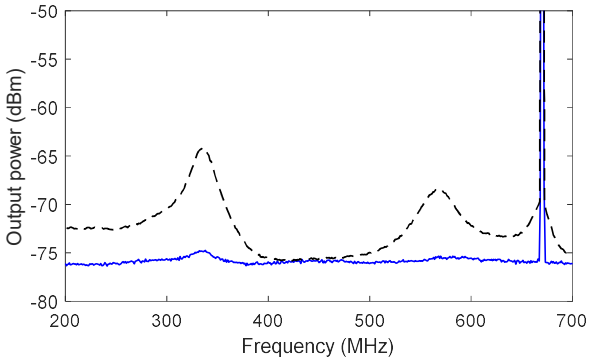

a)

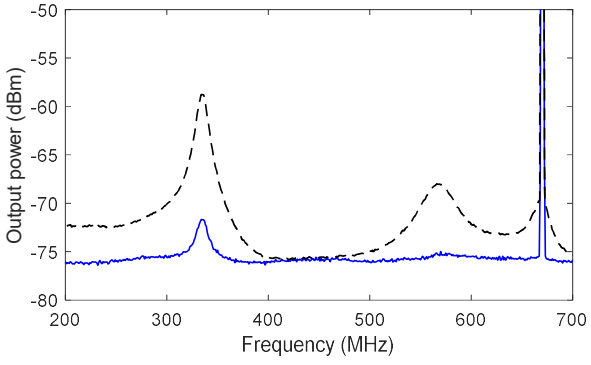

b)

Fig. 9. Comparison of output spectrum of conventional measurement without noise injection (solid line) and with -120 dBm/Hz injected noise (dashed line) for: a) P_{in} = 6 dBm: b) P_{in} = 9 dBm

Let us estimate now the critical poles of the divider circuit from the noise measurements using the methodology explained in section II.B. Those poles were originally identified using a reflective measurement with a VNA, following the technique in [7] (Fig. 6b). We apply now pole-zero identification to the noise traces shown in Fig. 8, which were obtained for different P_{in} levels. A null phase is considered along the frequency band. As an example, Fig. 10 shows the identification results for P_{in} = 2 dBm.

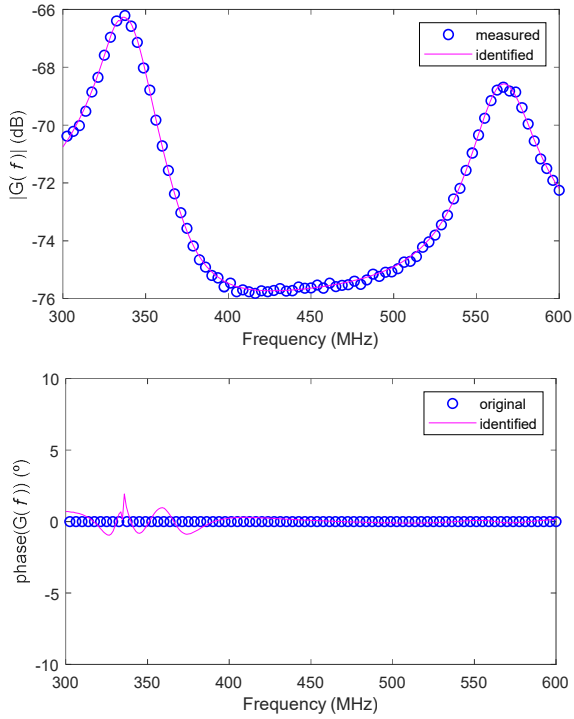

Fig. 10. Example of identification for the divider circuit. Identification results from the noise measurements corresponding to an input power at f_0 of 2 dBm. The phase values of the frequency response $G(f)$ are set to zero as in (7).

The poles obtained for the different P_{in} levels are shown in Fig. 11. As expected, symmetrical poles are obtained on the two half planes (LHP and RHP). However, as discussed in section II.B, we are only concerned with the LHP poles, the ones that represent the original system.

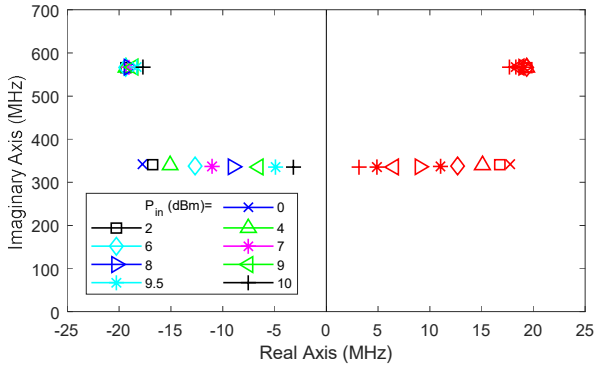

Fig. 11. Poles identified from noise measurements of the divider circuit given in Fig. 8. Only positive frequencies of the complex plane are plotted.

These LHP poles are superimposed in Fig. 12 to the ones from Fig. 6b, showing a good agreement that confirms the capability of the noise injection technique to estimate the dynamics of the circuit.

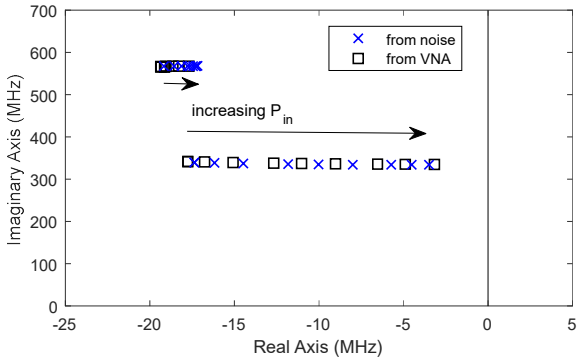

Fig. 12. Comparison between LHP poles of Fig. 11, identified from noise measurements (x), and poles given in Fig. 6b (square), identified from reflective measurements in a VNA.

B. *Amplifier*

The previous varactor-based frequency divider is a simple non-linear device that was well suited to illustrate the technique and validate the results because its critical poles could be characterized with an alternative technique. In this section, a second example will be presented. It is a medium power L-band amplifier based on a single GaAs FET (FLU17XM). When biased with V_{GG} = -2.1 V, V_{DD} = 2 V and driven with an RF signal at 1.2 GHz, this amplifier presents a low-frequency instability as a function of input power level. A photograph of the circuit is given in Fig. 13. The output spectrum for a P_{in} of 2 dBm is presented in Fig. 14, showing a spurious oscillation at almost 200 MHz and numerous intermodulation products.

Contrarily to the previous example, the RF ports of the amplifier are decoupled from low frequency. This is common in RF amplifiers due to the matching networks. Thus, techniques such as [7] cannot be directly used to measure the critical poles at the frequencies of the instability in this case because the lack of sensitivity. This lack of sensitivity will be illustrated later in this section. Instead, we will use CAD simulations to obtain the critical poles of the amplifier. The simulated poles will be used to validate the results of the noise injection technique.

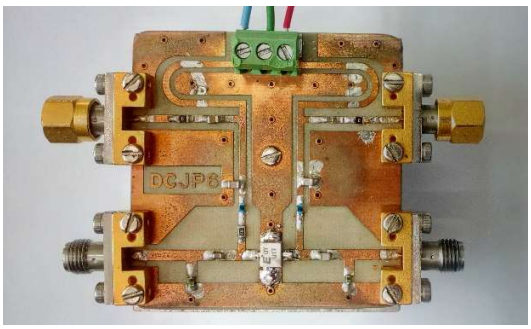

Fig. 13. Photograph of medium power L-band amplifier based on a single GaAs FET (FLU17XM), which presents a low-frequency instability as a function of input power level.

To obtain the critical poles from CAD simulations, pole-zero identification has been applied to an impedance frequency response calculated at an internal node of the circuit [31]. The poles obtained with input power from -4 to 5 dBm are given in Fig. 15. Again, poles corresponding to two resonances can be seen: one at about 240 MHz with poles moving leftwards with increasing input power and the other at almost 200 MHz moving rightwards and finally crossing to RHP. Note that there is a difference in the P_{in} value leading to instability between measurement and simulation. Experimentally, oscillation shows up for P_{in} = 2 dBm (Fig. 14), while simulation results predict it for P_{in} = 5 dBm.

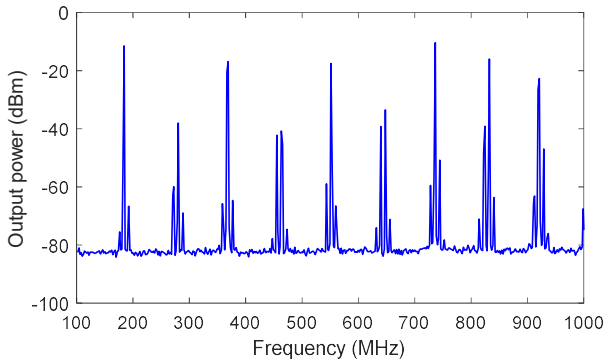

Fig. 14. Output spectrum of amplifier showing a spurious oscillation at almost 200 MHz and numerous intermodulation products (P_{in} = 2 dBm).

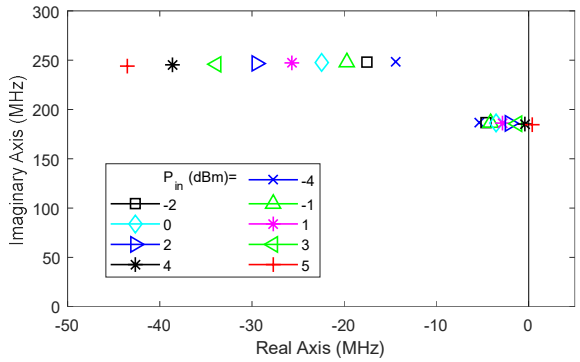

Fig. 15. Two pairs of complex conjugate dominant poles simulated with input power increasing from -4 to 5 dBm; the poles at 240 MHz move leftwards while the critical poles at 200 MHz move rightwards and cross to RHP.

Let us apply the noise injection technique to the amplifier biased as above, for an input power of -4 dBm. The resolution bandwidth of the spectrum analyzer is maintained at 1 MHz during all the characterization process. As shown in Fig. 16, without noise injection, i.e. only noise corresponding to a cold load, no hint of resonances is observed in the output spectrum at those frequencies (bottom trace in Fig. 16). However, injecting the broadband noise, the two resonances associated to the dominant poles can be revealed: one at 200 MHz and the other at 240 MHz, in good agreement with the poles shown in Fig. 15.

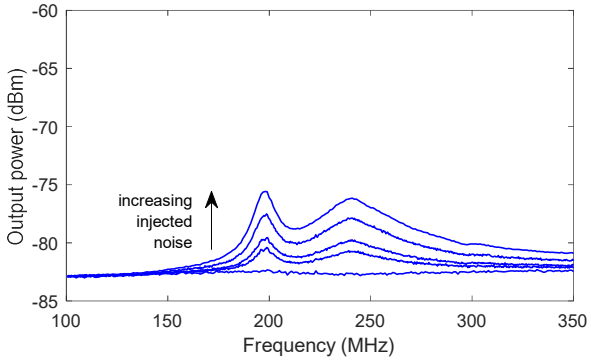

Fig. 16. Noise at the output of the amplifier, first measured without noise injection and then with four different levels of broadband noise (-98, -96, -93, -91 dBm/Hz), showing two resonances in good agreement with simulated poles.

For illustration, we have applied the method in [7] to the amplifier and compared results with the proposed technique. The magnitude of the complex admittance measured at the output port for an input power drive P_{in}=-4 dBm is plotted in Fig. 17 (right scale). Fig. 17 shows also the corresponding result when using the proposed technique based on injecting and measuring noise (left scale). The level of injected noise is -91 dBm/Hz. We can observe that the sensitivity to the critical resonances is notably improved in the proposed technique (note the significant difference in scales).

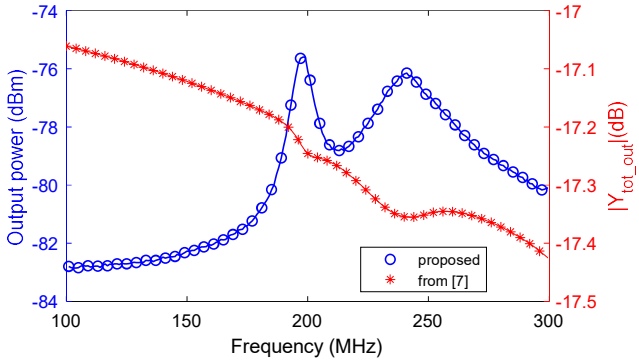

Fig. 17. Comparison of results for the GaAs FET amplifier, for P_{in} = -4 dBm, f_0 = 1.2 GHz, obtained with [7] (*, right scale) and with the proposed method (o, left scale).

To see the evolution of the resonances in Fig. 16, we can increase the power level of the input signal while the broadband noise is maintained at -91 dBm/Hz (ENR = 83 dB). The measurement results can be seen in Fig. 18. The resonance corresponding to the critical pole at 200 MHz increases notably and sharpens in relation with the resonance at 240 MHz. This is in agreement with the pole evolution of Fig. 15.

The effect of injecting broadband noise at the input of the circuit causes the observed noisy precursor to increase homogeneously (all the noise knoll raises equally), as expected. The effect can include a parametric amplification effect [26] and noise sideband conversions as in a regular mixer. This is observed in Fig. 16 for instance. The effect is different when the input drive is modified as in Fig. 18. An increase in P_{in} implies a new steady state, whose linearization has critical poles

with lower damping factor in this case. This means a narrower resonance with a higher peak. As the input power is increased, poles shift rightwards and the effect magnifies. This can be observed in the evolution of the noisy precursor at 200 MHz in Fig. 18. As P_{in} increases, the height of the peak raises and the width of the noise knoll narrows, in agreement with the reduction of the pole damping factor.

Again, it is important to highlight the need of noise injection to detect the resonances above the instrument noise floor. Fig. 19 shows a comparison of the output spectrum measurements with and without noise injection for an input power of 1 dBm, i.e. very close to the bifurcation point. Although small, a noisy precursor is visible in the cold measurement (solid line) thanks to the proximity of the bifurcation. The noise bumps observed with the noise injection technique (dashed line) are significantly bigger and will be above the noise floor no matter the configuration of the receiver of the spectrum analyzer (input attenuation, resolution bandwidth).

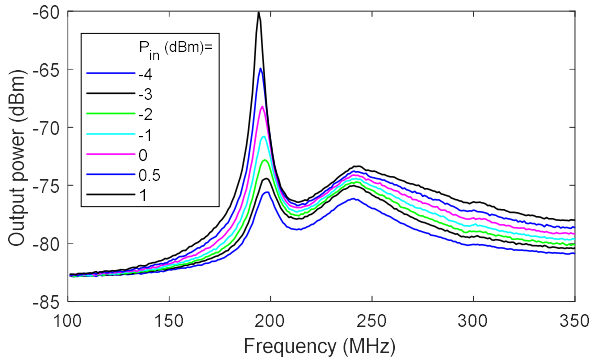

Fig. 18. Noise at the output of the amplifier for increasing input power from -4 to 1 dBm with a constant broadband noise of -91 dBm/Hz.

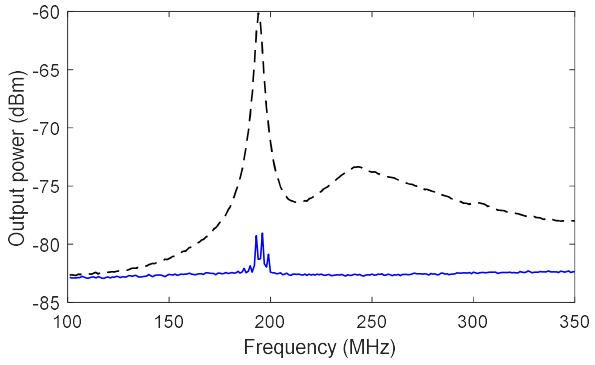

Fig. 19. Comparison of output noise with input noise of -91 dBm/Hz (dashed line) and without noise injection (solid line), for an input power of 1 dBm.

As in the previous case, we can now obtain the critical poles of the amplifier from the noise measurements of Fig. 18. The obtained results are shown in Fig. 20, where the symmetrical RHP poles have been eliminated. These poles are compared in Fig. 21 with the poles identified from simulations of Fig. 15 (only simulations up to 1 dBm have been depicted to facilitate comparison).

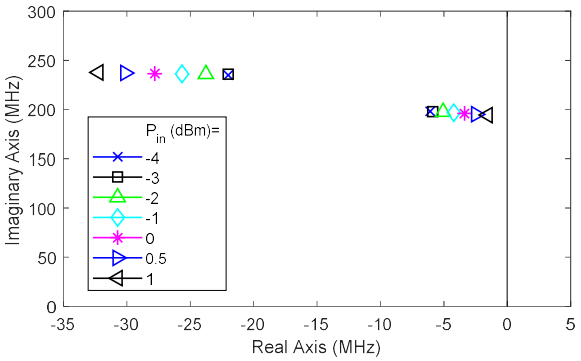

Fig. 20. Poles identified from noise measurements of the amplifier shown in Fig. 18. Only positive frequencies of LHP poles are plotted.

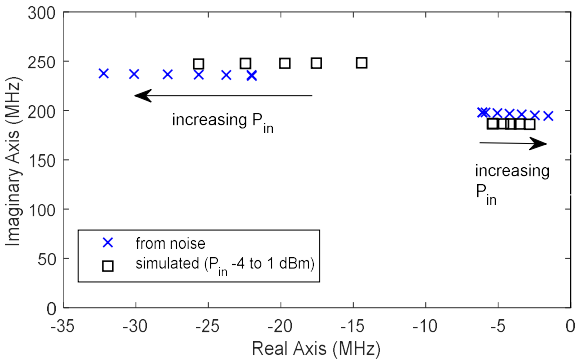

Fig. 21. Poles of Fig. 20 compared to simulated poles of Fig. 15 (only those corresponding to P_{in} up to 1 dBm). Despite the qualitative agreement, there are some quantitative differences. It should be reminded that simulation predicted instability for a P_{in} of 5 dBm, however the circuit is actually unstable for an input power of 2 dBm, as shown in Fig. 14.

As it can be seen, although there is qualitative agreement, there are some quantitative differences: in addition to a few MHz difference in frequency, the critical poles from measurements get closer to the RHP than the simulated ones, while the poles at 240 MHz are farther. Measured poles are consistent with the experimental behavior of the amplifier that shows an oscillation for P_{in} = 2 dBm (Fig. 14), while simulation predicted the oscillation for P_{in} = 5 dBm.

It is important to outline that the level of the injected broadband noise can affect the identification of the critical poles. Too large levels of injected noise can modify the steady state of the circuit, which should be governed only by the large-signal input power P_{in}. In that case, the obtained frequency response does not represent a linearized system anymore and some errors in the identification results should be expected. However, although the position of the poles could not be accurately obtained on the complex plane, the presence of noisy precursors would still reveal the critical resonances.

V. Discussion and Practical Limitations

The previous results have shown that the injection of broadband noise can be applied to circuits operating in large signal in order to detect the presence of critical resonances and assess stability margins from the position of the corresponding poles on the complex plane.

The proposed technique has some benefits with respect to previous techniques [7], [18], [19] to characterize the critical poles of an amplifier in large-signal. Firstly, it has the simplicity of a scalar characterization technique, contrarily to the vector characterization required by previous techniques. Techniques in [18] and [19] are only applicable to low frequency resonances, as explained in the introduction. The technique in [7] has the drawback of having low sensitivity to critical resonances outside the operating band of the amplifier.

Increasing the level of the noisy precursors has also the benefit of relaxing the noise floor requirements of the setup receiver. This is important in this type of measurements, in which the circuit is operating in large signal at the fundamental frequency while linear measurements are carried out at some other frequencies. If the DUT is a high-power amplifier, the receiver may undergo a very large tone at the fundamental frequency, compromising the linearity of the receiver if no input attenuation is used. This is a problem for [7], which uses a VNA as receiver, since attenuation will affect the sensitivity of the S-parameter measurement. In our case, receiver linearity can be easily attained increasing the input attenuation of the spectrum analyzer, which in turn raises the receiver noise floor. Enhancing the level of the noisy precursors allows their observation over the noise floor for SA settings (input attenuation) that are compatible with the preservation of receiver linearity.

Another benefit of enhancing the noisy precursors is related to the frequency response resolution required to identify the critical poles. If, in the absence of injected noise, the level of the noisy precursor (per Hertz) is of the order of the receiver noise floor (per Hertz) the use of a wide resolution bandwidth (RBW) does not provide enough resolution to identify the shape of the noisy precursor. In the worst case, we may miss the presence of the noisy precursor. However, if the injection of noise raises the noise bump high enough above the noise floor, the wide RBW can now be used to detect the precursor clearly and identify the position of the critical poles.

The proposed approach also presents some limitations. As it is noted in [3], the observability of the noisy precursors in the spectrum also depends on the form of the pole evolution with the circuit parameters. Poles need to remain close to the axis in a certain interval of the input drive P_{in}. If under small P_{in} variations the magnitude of the real part of the critical poles $|\sigma_d|$ evolve quickly, the noisy precursors will be hardly observable.

Characterization of DUTs with very high noise figure may also present a practical drawback. If, at some frequency bands, the input/output gain of the DUT is extremely low (which directly entails a very high noise figure) the broadband injected noise may be so attenuated that it does not contribute to the increase of the noisy precursors. Despite this, if the added noise generated by the DUT´s internal noise sources is large enough, noisy precursors might still be observable. Additionally, even if DUT attenuation is large in a certain bandwidth, the noise conversion from other side bands can still contribute to the observability of noisy precursors (note that the broadband noise is mixed with the large-signal input). This is the advantage of exciting the DUT with a broadband noise source that covers simultaneously all the measurement bandwidth.

Alternatively, we could modify the measurement setup by substituting the injected broadband noise by a level-controlled CW source that is swept in frequency. The method to obtain the poles from scalar measurements is also applicable in this case. The main downside with respect to the broadband noise excitation is that we lose the benefit of converting noise from different sidebands.

VI. Conclusion

An undemanding technique has been proposed to characterize the critical dynamics of non-linear RF circuits. Broadband noise is injected at the input of the circuit and the output is measured with a spectrum analyzer. Thanks to the noise injection, noise-bumps associated to critical resonances are made visible above the instrument noise floor without exigent measurement settings and without the need of reaching bifurcation point. The technique has the potential to be used as a diagnostic tool for amplifier robustness in terms of stability margins. Moreover, the location of the critical poles can be estimated from the noise measurements, applying pole-zero identification techniques.

References

[1] S. C. Cripps, *RF Power Amplifiers for Wireless Communications*, 2nd Edition, Artech House, 2007.

[2] A. Grebennikov, K. Narendra, and B. S. Yarman, *Broadband RF and Microwave Amplifiers*, 1st ed. New York: CRC Press, 2016.

[3] A. Suárez, *Analysis and Design of Autonomous Microwave Circuits*. New York: Wiley, 2009.

[4] A. Suárez, "Check the Stability: Stability Analysis Methods for Microwave Circuits," *IEEE Microw. Mag.*, vol. 16, no. 5, pp. 69 – 90, May 2015, doi: 10.1109/MMM.2015.2410951

[5] S. Rumery, and B. Noori, "A new technique for measuring the resonant behavior of power amplifier bias circuits," in *69th ARFTG Conf.,* Honolulu, HI, Jun. 2007, pp. 1-9.

[6] S. Schaffer, Z. Popovic, "Multi-Frequency Measurements for Supply Modulated Transmitters", *IEEE Trans. Microw. Theory Techn.*, vol. 63, no. 9, pp. 2931-2941, September 2015, doi: 10.1109/TMTT.2015.2458962

[7] N. Otegi, A. Anakabe, J. Pelaz, J. M. Collantes, and G. Soubercaze-Pun, "Experimental characterization of stability margins in microwave amplifiers," *IEEE Trans. Microw. Theory Techn.*, vol. 60, no. 12, pp 4145-4156, Dec. 2012, doi: 10.1109/TMTT.2012.2221736

[8] C. T. Rodenbeck, M. M. Elsbury, J. W. Dimsdle, "Techniques for the analysis and elimination of transient oscillations in wideband and ultra-wideband pulsed power amplifiers," *IEEE Trans. Microw. Theory Techn.*, vol. 61, no. 10, pp. 3733-3742, Oct. 2013, doi: 10.1109/TMTT.2013.2280114

[9] H. H. Ladhani, J. K. Jones, and G. Bouisse, "Improvements in the instantaneous-bandwidth capability of RF Power Transistors using in-package high-k capacitors," in *IEEE MTT-S Int. Microw. Symp. Dig.*, Baltimore, MD, USA, Jun. 2011, pp. 1-4, doi: 10.1109/MWSYM.2011.5972860

[10] I. Takenaka and K. Ishikura; H. Takahashi; K. Hasegawa; K. Asano; N. Iwata, "Improvement of Intermodulation Distortion Asymmetry Characteristics With Wideband Microwave Signals in High Power Amplifiers," *IEEE Trans. Microw. Theory Techn.*, vol. 56, no. 6, pp. 1355-1363, Jun. 2008, doi: 10.1109/TMTT.2008.923365

[11] R. C. Melville, A. Suárez, "Experimental Investigation of Bifurcation Behavior in Nonlinear Microwave Circuits," *IEEE Trans. Microw. Theory Techn.*, vol. 65, no. 5, pp. 1545-1559, May 2017, doi: 10.1109/TMTT.2016.2640955

[12] C. Florian, P. A. Traverso, A. Santarelli, F. Filicori, "An Active Bias Network for the Characterization of Low-Frequency Dispersion in High-

Power Microwave Electron Devices", *IEEE Trans. Instrum. Meas.*, vol. 62, no. 10, pp. 2857-2869, Oct. 2013, doi: 10.1109/TIM.2013.2263911
[13] G. P. Gibiino, J. Couvidat, G. Avolio, D. Schreurs, A. Santarelli, "Supply-Terminal 40 MHz BW Characterization of Impedance-like Nonlinear Functions for Envelope Tracking PAs," in *87th ARFTG Microwave Measurement Conference,* San Francisco, CA, USA, May 2016, doi: 10.1109/ARFTG.2016.7501958
[14] X. Perpiñà, F. Reverter, J. Leon, E. Barajas, M. Vellvehí, X. Jordà, J. Altet, "Output Power and Gain Monitoring in RF CMOS Class A Power Amplifiers by Thermal Imaging," *IEEE Trans. Instrum. Meas.*, vol. 68, no. 8, pp. 2861-2870, August 2019, doi: 10.1109/TIM.2018.2871289
[15] W.S. El-Deeb, N. Boulejfen, F.M. Ghannouchi, "A Multiport Measurement System for Complex Distortion Measurements of Nonlinear Microwave Systems," *IEEE Trans. Instrum. Meas.*, vol. 59, no. 5, pp. 1406-1413, May 2010, doi: 10.1109/TIM.2010.2045033
[16] R. Pintelon, E. Louarroudi, J. Lataire, "Time-Variant Frequency Response Function Measurements on Weakly Nonlinear, Arbitrarily Time-Varying Systems Excited by Periodic Inputs," *IEEE Trans. Instrum. Meas.*, vol. 64, no. 10, pp. 2829-2837, Oct. 2015, doi: 10.1109/TIM.2015.2426351
[17] E. Louarroudi, R. Pintelon, J. Lataire, "Nonparametric Tracking of the Time-Varying Dynamics of Weakly Nonlinear Periodically Time-Varying Systems Using Periodic Inputs," *IEEE Trans. Instrum. Meas.*, vol. 61, no. 5, pp. 1384-1394, May 2012, doi: 10.1109/TIM.2011.2175830
[18] J. Pelaz, J. M. Collantes, N. Otegi, A. Anakabe, G. Collins "Experimental Control and Design of Low-Frequency Bias Networks for Dynamically Biased Amplifiers," *IEEE Trans. Microw. Theory Techn.*, vol. 63, no. 6, pp. 1923-1936, Jun. 2015, doi: 10.1109/TMTT.2015.2419213
[19] JM. Gonzalez, N. Otegi, A. Anakabe, L. Mori, A. Barcenilla, JM. Collantes, "In-Circuit Characterization of Low-Frequency Stability Margins in Power Amplifiers", *IEEE Trans. Microw. Theory Techn.*, vol. 67, pp. 822 – 833, Feb. 2019, doi: 10.1109/TMTT.2018.2883568
[20] J. Urbonas, K. Kim, P. H. Aaen, "Direct E-Field Measurement and Imaging of Oscillations within Power Amplifiers," *IEEE Trans. Instrum. Meas.*, fol. 68, No. 8, pp. 2971-2978, August 2019, doi: 10.1109/TIM.2018.2869407
[21] J. Urbonas, K. Kim, F. Vanaberbeke, P. H. Aaen, "An Electro-Optic Pulsed NVNA Load–Pull System for Distributed E-Field Measurements," *IEEE Trans. Microw. Theory Techn.*, vol. 66, No. 6, pp. 2896-2903, June 2018, doi: 10.1109/TMTT.2018.2816930
[22] J. Jeffries and K. Wiesenfeld, "Observation of noisy precursors of dynamical instabilities," *Phys. Rev. A, Gen. Phys.*, vol. 31, no. 2, pp. 1077-1084, Feb. 1985, doi: https://doi.org/10.1103/PhysRevA.31.1077
[23] S. Jeon, A. Suárez, and R. Rutledge, "Analysis and elimination of hysteresis and noisy precursors in power amplifiers," *IEEE Trans. Microw. Theory Techn.*, vol. 54, no. 3, pp. 1096-1106, Mar. 2006, doi: 10.1109/TMTT.2005.864125
[24] J. M. Collantes, I. Lizarraga, A. Anakabe, and J. Jugo, "Stability verification of microwave circuits through Floquet multiplier analysis," in *IEEE APCCAS*, Tainan, Taiwan, Dec. 2004, pp. 997–1000, doi: 10.1109/APCCAS.2004.1413049
[25] F. Bonani and M. Gilli, "Analysis of Stability and Bifurcations of Limit Cycles in Chuas's Circuit through the Harmonic-Balance Approach", *IEEE Trans. Circuits Syst. I, Fundam. Theory App.*, vol. 46, no. 8, pp. 881-890, August 1999, doi: 10.1109/81.780370
[26] F. X. Kaertner, "Analysis of white and f$^{-\alpha}$ noise in oscillators," *Int. J. Circuit Theory Appl.*, vol. 18, pp.485-519, 1990
[27] J. M. Collantes, L. Mori, A. Anakabe, N. Otegi, I. Lizarraga, N. Ayllon, F. Ramírez, V. Armengaud, G. Soubercaze-Pun, "Pole-Zero Identification: Unveiling the Critical Dynamics of Microwave Circuits Beyond Stability Analysis," *IEEE Microw. Mag.*, vol. 20, no. 7, pp. 36-54, July 2019, doi: 10.1109/MMM.2019.2909516
[28] F. Iturbide-Sanchez, S.C. Reising, S. Padmanabhan, "A Miniaturized Spectrometer Radiometer Based on MMIC Technology for Tropospheric Water Vapor Profiling," IEEE *Trans Geosci Remote Sens*, vol. 45, no. 7, pp. 2181-2194, July 2007, doi: 10.1109/TGRS.2007.898444
[29] A. El-Sharkawy, P. P. Sotiriadis, P. A. Bottomley, E. Atalar, "Absolute Temperature Monitoring Using RF Radiometry in the MRI Scanner," *IEEE Trans. Circuits Syst. I, Reg. Papers*, vol. 53, no. 11, pp. 2396-2404, Nov. 2006, doi: 10.1109/TCSI.2006.884423
[30] IVCAD – STAN Tool. AMCAD Engineering, Limoges, France, 2013. Accessed on: March 23, 2022. [Online]. Available: https://www.amcad-engineering.com/software-module/stan
[31] N. Ayllon, A. Anakabe, J.M. Collantes, G. Soubercaze-Pun, S. Forestier, "Sensitivity enhancement in pole-zero identification based stability analysis of microwave circuits," *in Integr. Nonlinear Microw. Millim.-Wave Circuits Workshop*, Malaga, Spain, Nov. 2008, pp. 75-78, doi: 10.1109/INMMIC.2008.4745719

Nerea Otegi received the Ph.D. degree from the University of the Basque Country (UPV/EHU), Bilbao, Spain, in 2008. In 2002, she joined the Electricity and Electronics Department, UPV/EHU, where she has been an Associate Professor since 2006. Her areas of interest include noise characterization at microwave frequencies and nonlinear analysis of microwave circuits.

Juan-Mari Collantes received the Ph.D. degree in electronics from the University of Limoges, France, in 1996. He became an Associate and Full Professor of Electronics with the Electricity and Electronics Department, University of the Basque Country (UPV/EHU), Bilbao, Spain, in 1996 and 2019, respectively. In 1996 and 1998 he was an Invited Researcher with Agilent Technologies (formerly the Hewlett-Packard Company), Santa Rosa, CA. In 2003, he was with the French Space Agency (CNES), Toulouse, France, where he was involved with power amplifier analysis, simulation, and modelling. His areas of interest include nonlinear analysis and design of microwave circuits, microwave measurement techniques and noise characterization.

Ibone Lizarraga received the M.Sc. degree in physics with electronics and Ph.D. degree in control engineering from the University of the Basque Country (UPV/EHU), Bilbao, Spain, in 1994 and 2001, respectively. She is currently with the Electricity and Electronics Department, UPV/EHU, where she has been an Associate Professor since 1998. Her research interests include the analysis and control of mechatronic system, stability analysis and linear and nonlinear system identification.

Jose Manuel Gonzalez received the M.Sc. degree from ENSEEIHT, Toulouse, France, in 2008, and the Ph.D. degree in high-frequency electronics from the Université de Limoges, France, and Carleton University, Ottawa, Canada, in 2011. In 2012 he joined KAUST (Saudi Arabia) as a Post-Doctoral Researcher. In 2015, he joined the Electricity and Electronics Department, UPV/EHU as a Post-Doctoral Researcher and since 2017 he is an Adjunct Professor in the

Electronic Technology Department (UPV/EHU). His areas of interest are experimental characterization of magnetic materials, in-circuit measurements and EM simulation.